Supplementary Information

Magnetic-assisted alignment of nanofibers in polymer nanocomposite for high-temperature capacitive energy storage applications

Zhi Li[a], Jian Wang[a], Junjie Zou[a], Shuxuan Li[a], Xin Zhen[a], Zhonghui Shen[a], Baowen Li[a], Xin Zhang[*a] and Ce-Wen Nan[*b]

a State Key Laboratory of Advanced Technology for Materials Synthesis and Processing, Center of Smart Materials and Devices, Wuhan University of Technology, Wuhan, Hubei, China

b Address School of Materials Science and Engineering, State Key Lab of New Ceramics and Fine Processing, Tsinghua University, Beijing, 100000, China

E-mail address: zhang-xin@whut.edu.cn (Xin Zhang), cwnan@tsinghua.edu.cn (Ce-Wen Nan)

Experimental Section

Modified Electrospinning process: The difunctional FTO nanofibers were obtained through a modified electrospinning process, the prepared sol was transferred into a syringe equipped with a metal needle, the positive high voltage applied to the needle was carefully controlled at 10 kV, while the negative high voltage applied to the collector was set at -3 kV. The distance between the needle and the collector was maintained at 30 cm. The flow rate was adjusted to 1 ml/h for 20 ml syringe. The temperature and humidity were kept at 30 °C and below 30%. A magneton was added into the syringe with the sol, and a rotating magnetic field was applied to synchronize the processes of mixing and electrospinning.

Structural Characterization: The morphology of FTO nanofibers, as well as the surface and cross-sectional morphology of polymer nanocomposite films, were characterized using scanning electron microscopy (SEM) (JSM-7610FPLUS, JEOL, Japan) and energy-dispersive X-ray spectroscopy (EDS) (Smartedx Oxford). The crystal structures of calcined composite nanofibers and composite films were analyzed with X-ray diffraction (XRD) (SmartLab, Rigaku, Japan) using a Cu Kα source. X-ray photoelectron spectroscopy (XPS) analysis was conducted using an ESCALAB 250Xi spectroscopy with an Al Kα source. Ultraviolet photoelectron spectroscopy (UPS) was carried out on an ESCALAB 250Xi with He-I lamp radiation (21.2 eV), and the Fermi level was calibrated using clean Cu. The work function was calculated based on the binding energy of the secondary electron edge (E_{SEE}) (φ = 21.2 eV - E_{SEE}).

Dielectric Properties Characterization: The dielectric data were characterized using a dielectric temperature measuring oven (PK-CPT1705, 25-250 °C) in conjunction with an impedance analyzer (Agilent 4294A, 10^2-10^6 Hz) with a clamp (Agilent 16034G), the electric displacement-electric field (D-E) loops and DC leakage current density-electric field (I-V) curves of the samples were measured by a ferroelectric test system (Premier II, Radiant Technologies, Inc.), where the samples were soaked in silicon dielectric fluid, the temperature was controlled utilizing a digital hot plate equipped with a thermal couple. Dielectric breakdown strengths were measured by a Dielectric Withstand Voltage Test System (Beijing Electro-mechanical Research Institute Super-voltage Technique), the temperature ramping rate and limit leakage current were set as 200 V/s and 4 mA, respectively. The cyclic fast charge-discharge test was performed using a PK-CPR-1901 test system (Polyk Technologies),

Isothermal Surface Potential Decay (ISPD) Measurement

The ISPD measurement was measurement by Trek 341B surface potentiometer, before the test, the sample with corona discharge method (bias voltage -15 kV and -6 kV) was used to charge the surface of the samples, after being charged for 10 min, the sample was quickly moved below the Kelvin probe (Trek 341B) to record the variation of surface potential at constant temperature (50 °C) for 30,000 s.

The trap energy level (E_T)and trap energy density (Q_T) can be ascribed as

$$E_T = K_B T ln(vt) \quad (1)$$

$$Q_T = t \frac{\varepsilon_0 \varepsilon_r}{eM} \frac{d\varphi(t)}{dt} \quad (2)$$

Where v is the escape frequence, t is escape time, $\varphi(t)$ is surface potential, M is the thickness of the composite films.

Pulse Electro Acoustic (PEA) Measurement

The characterization of charge injection from the electrodes into the dielectrics was carried out by pulse electro acoustic (PEA) method at high temperature and high electric fields. The sample was placed in a constant temperature oven, with a external electric pulse applied on it, the time duration is 200 s. Then a force was applied at the sample, with acoustic wave assumed to propagate occur along x axis, the space charge distribution was assumed that force acting on a space charge density within the sample assembly couple rigidly to the surrounding polymer and electrodes, and the electric pulse is an impulse with a very narrow duration. The spatial resolution is limited by the thickness of the sensor (7 μm), polymer-based composite films with the thickness of about 200 μm were used in PEA measurement.

The net space charge distribution $\partial_{n\,(x,t)}$ is defined as the injection charges excluding the image charge at the electrodes:

$$\partial_{n(x,t)} = \partial_{(x,t)} - \partial_{(x,0)} \quad (3)$$

and the average net charge density q_t is defined as:

$$q_t = \frac{1}{d} \int_0^d \left| \partial_{n(x,t)} \right| dx \quad (4)$$

where d is the thickness of the samples.

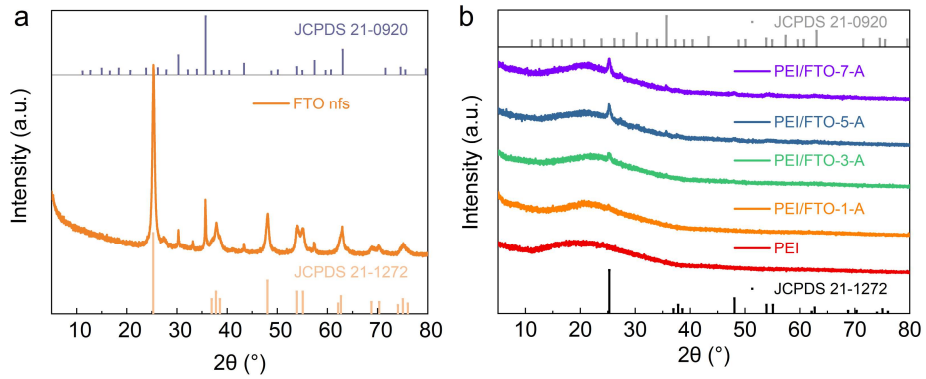

Fig. S1 XRD of the a) composite FTO nfs and b) PEI/FTO composite films.

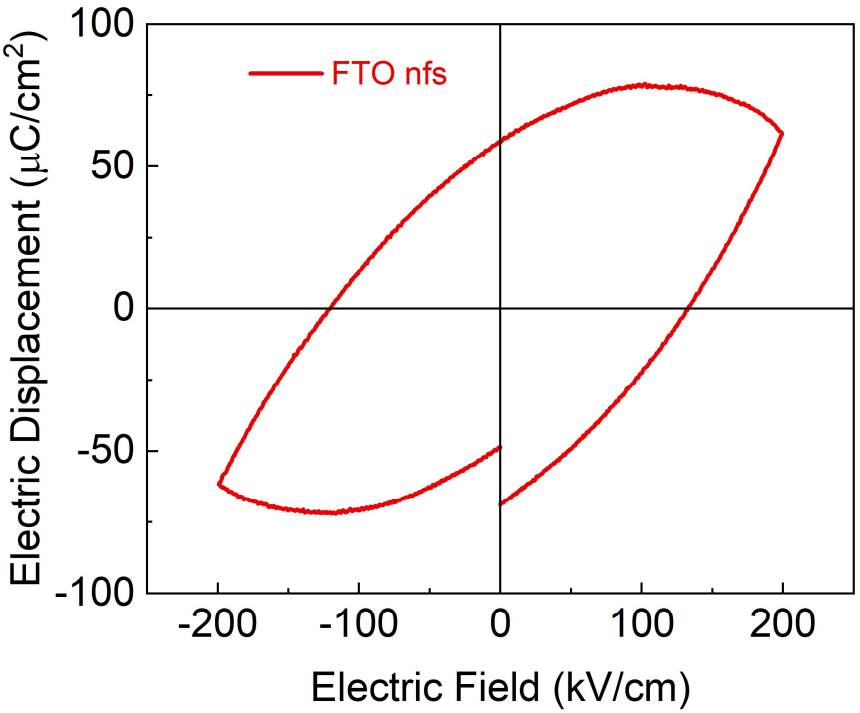

Fig. S2 Electric displacement-electric field loop of FTO nfs.

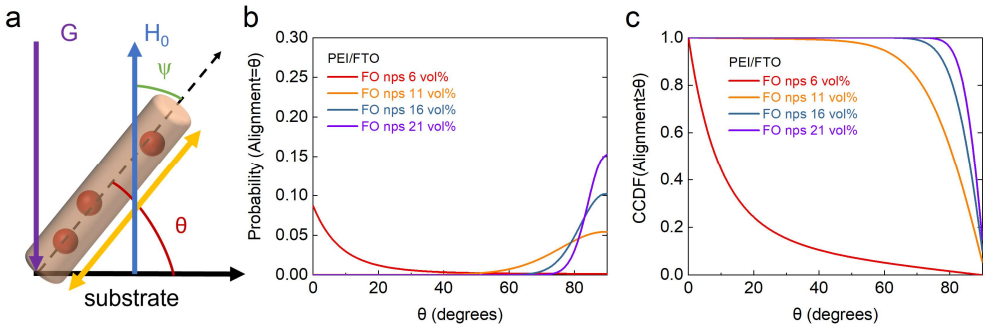

Fig. S3 a) Schematic illustration of FTO nfs in gravitational and magnetic fields; b) Theoretical probability of FTO nfs with 6, 11, 16 and 21 vol% FO nps rotated angles in PEI matrix under gravitational and magnetic fields; c) Complementary cumulative distribution function (CCDF) of FTO nfs in PEI matrix.

Orientational Calculation: The alignment of difunctional FTO nfs was served by the magnetic (U_m) and gravitational (U_g) potential energy and internal thermal energy,[1,2] the energy can be obtained by assuming that a fiber has a common prolate spheroidal model, the stored magnetic potential energy decreases with the angular displacement ψ, U_m can be ascribed as:

$$U_m = \frac{\pi L D^2 f \mu_m (\mu_f - \mu_m)^2 (G_D - G_L) H^2 sin^2\psi}{3[\mu_m - (\mu_m - \mu_f)G_D][\mu_m - (\mu_m - \mu_f)G_L]} \quad (5)$$

where D and L are the diameter and length of the FTO nfs, μ_m and μ_f are the magnetic permeability of the polymer matrices and fibers, respectively. μ_m is equal to the free space permeability μ_0, *i.e.*, $\mu_m=\mu_0=4\pi\times10^{-7}$ m kg/S^{2}A^2 and $\mu_f=\mu_0(\chi_f+1)$, χ_f is the magnetic susceptibility. G_D and G_L are geometry demagnetizing coefficients, when aspect ratio L/D exceeds 10, G_D and G_L can be estimated with numerical values as G_L=0.5 and G_D=0,[3] respectively. θ is the angle between the long axis of the fiber and the substrate plane, with the relation $\theta+\psi=90°$. Thus, U_m can be simplified as:

$$U_m = \frac{\pi L D^2 f \mu_0 \chi_f^2 H^2}{3(\chi_f+2)} sin^2(\frac{\pi}{2} - \theta) \quad (6)$$

The U_g of the nanofibers can be described as follow:

$$U_g = V_f(\rho_f - \rho_m) g \frac{L}{2} sin\theta \quad (7)$$

where V_f is the volume of composite fibers; ρ_f and ρ_m represent the density of the nanofibers and the polymer matrix solution, respectively; g is the gravitational constant. A canonical partition function, C, is used to describe the possible energy states of the fibers with Boltzmann statistics. When angle θ changes from 0° to 90°, C can be determined as follows:

$$C = \int_{0^\circ}^{90^\circ} e^{\frac{[-U_m(\psi)-U_g(\theta)]}{k_B T}} d\theta \quad (8)$$

The value of C represents the statistics of all possible energy states of the fibers under a certain magnetic field. We can integrate the canonical partition function over a certain degree versus the value of C to obtain the probabilities of fiber alignment from θ_1 to θ_2. The probabilities can be calculated as follows:

$$P_{\theta_1-\theta_2} = \frac{\int_{\theta_1}^{\theta_2} e^{\frac{[-U_m(\psi)-U_g(\theta)]}{k_B T}} d\theta}{C} \quad (9)$$

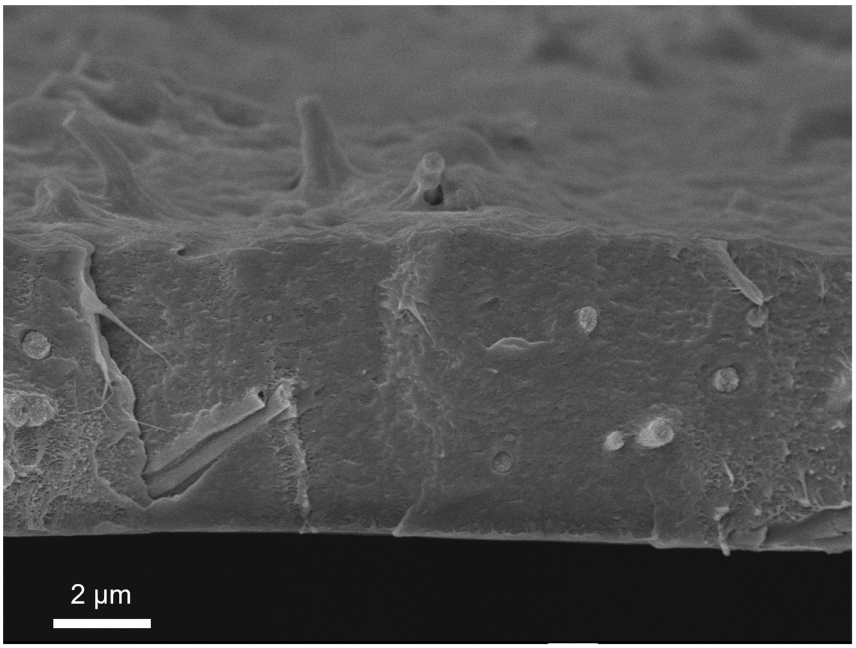

Fig. S4 SEM image of FTO nfs protrude from the PEI surface.

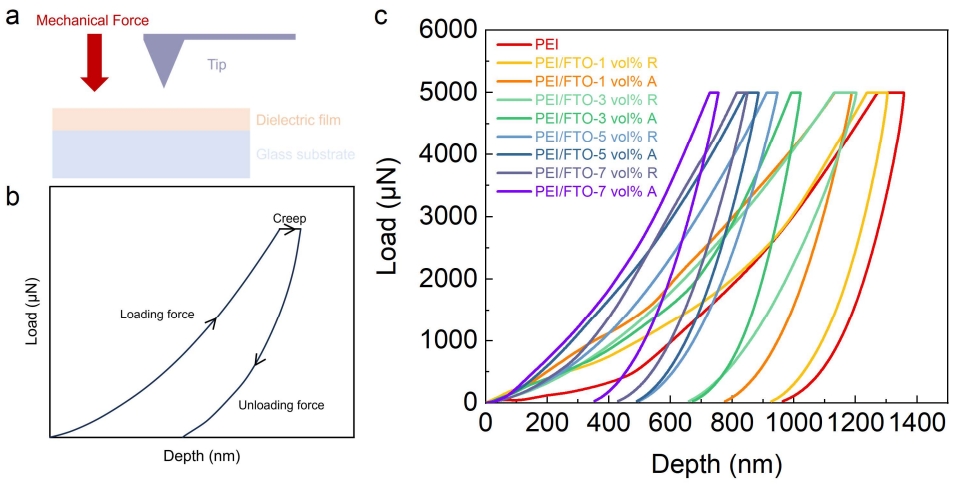

Fig. S5 a) Schematic illustration of nanoindentation method, b) The typical load-depth curve by nanoindentation; c) the load-depth curves of PEI/FTO composite films with different filler contents and nanofiber special orientation.

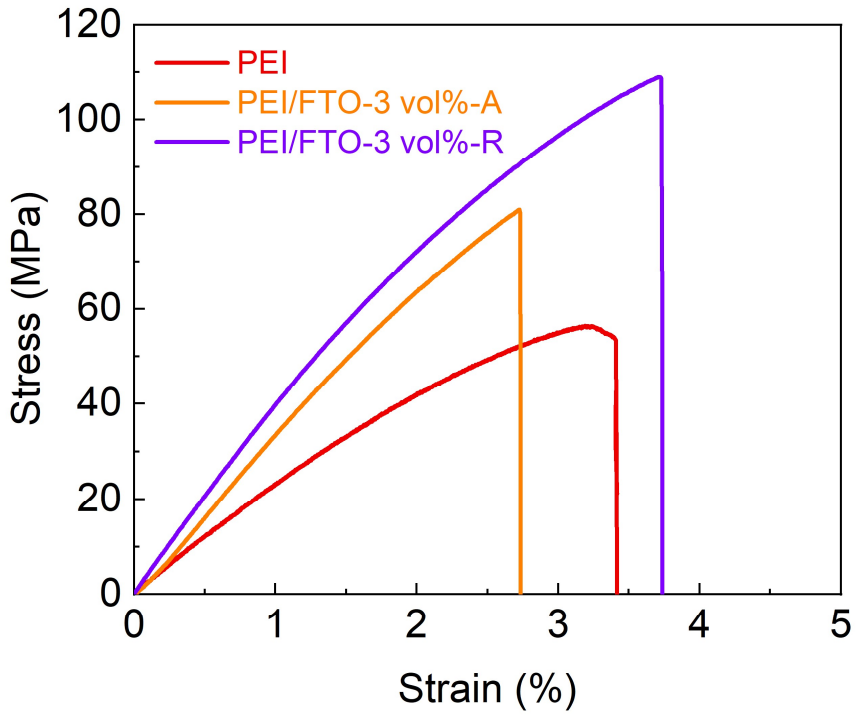

Fig. S6 Tensile strain-stress loops of PEI-matrix films composite with 3 vol% FTO nfs in different states.

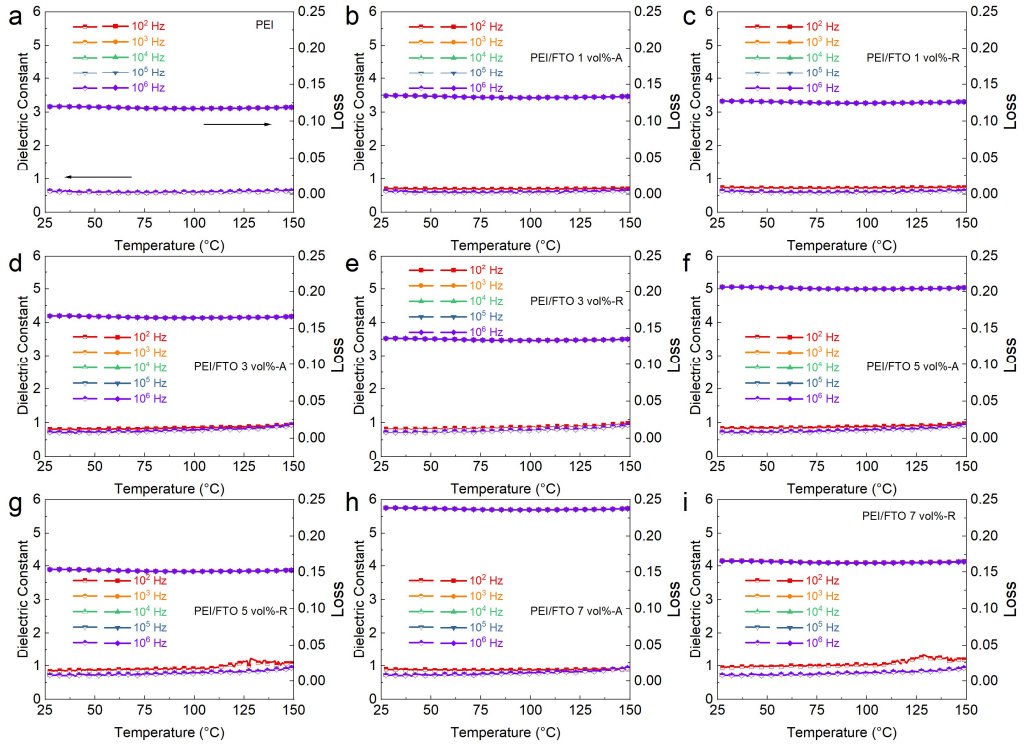

Fig. S7 Dielectric properties as a function of temperature and frequence spectrum of PEI/FTO composite films, temperature ranges from 25-150 °C, frequence were set at 10^2, 10^3, 10^4, 10^5 and 10^6 Hz.

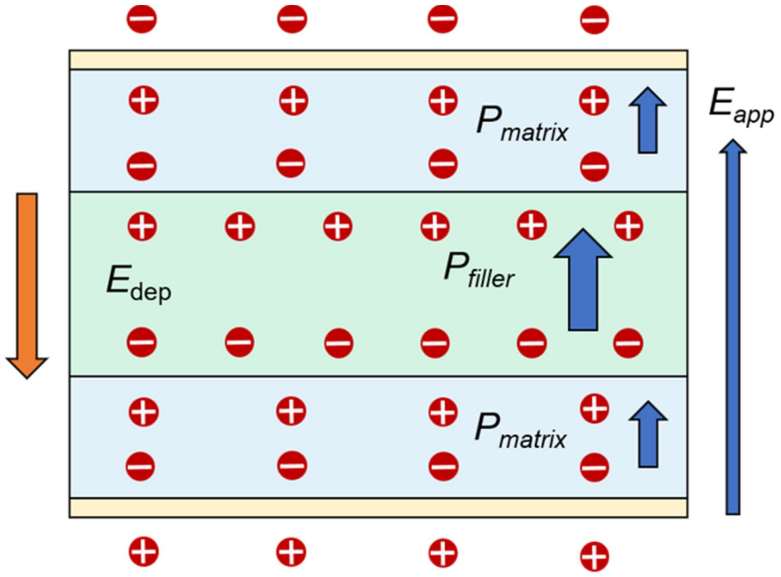

Fig. S8 Schematic illustration of polarization model.

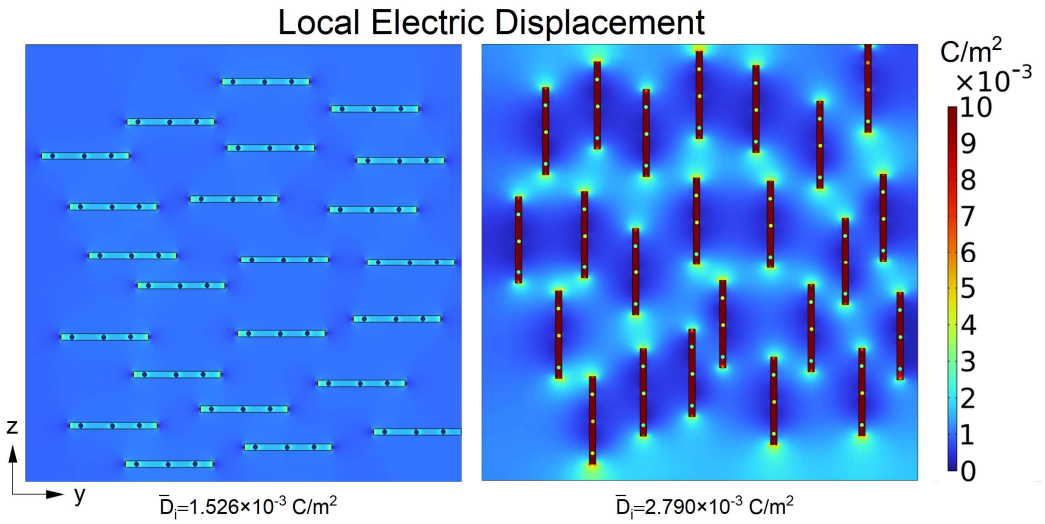

Fig. S9 Displacement distribution simulation of PEI-matrix composite film with 7 vol% different fiber orientation states FTO nfs at an electric field of 50 MV/m.

Simulation: Based on the experimentally observed microstructures, we designed two nanocomposites filled with nanofibers having specific ideal orientation angles of 0 and 90°. The 0.1−1.5 nanofibers represent nanofibers with a diameter of 0.1l and a length of 1.5l. The dielectric region is set as 10l×10l, and the content of nanofibers is set to 7 vol %. To investigate the effect of nanofiber orientation on the local distributions of polarization and then obtain the effective dielectric constant in nanocomposite films, the following electrostatic Poisson equation is solved:

$$\nabla \cdot D(r) = \nabla \cdot (\varepsilon_0 \varepsilon(r) E(r)) = \rho(r) \tag{10}$$

where $D(r)$ is the electric displacement, ε_0 is the vacuum permittivity, $\varepsilon(r)$ is the relative permittivity, $E(r)$ is the electric field, and $\rho(r)$ is the space charge density.

Then the effective dielectric constant tensor ε_{ij} could be calculated by:

$$\bar{D}_\iota = \varepsilon_0 \varepsilon_{ij} \bar{E}_J \tag{11}$$

where - represent the average value.

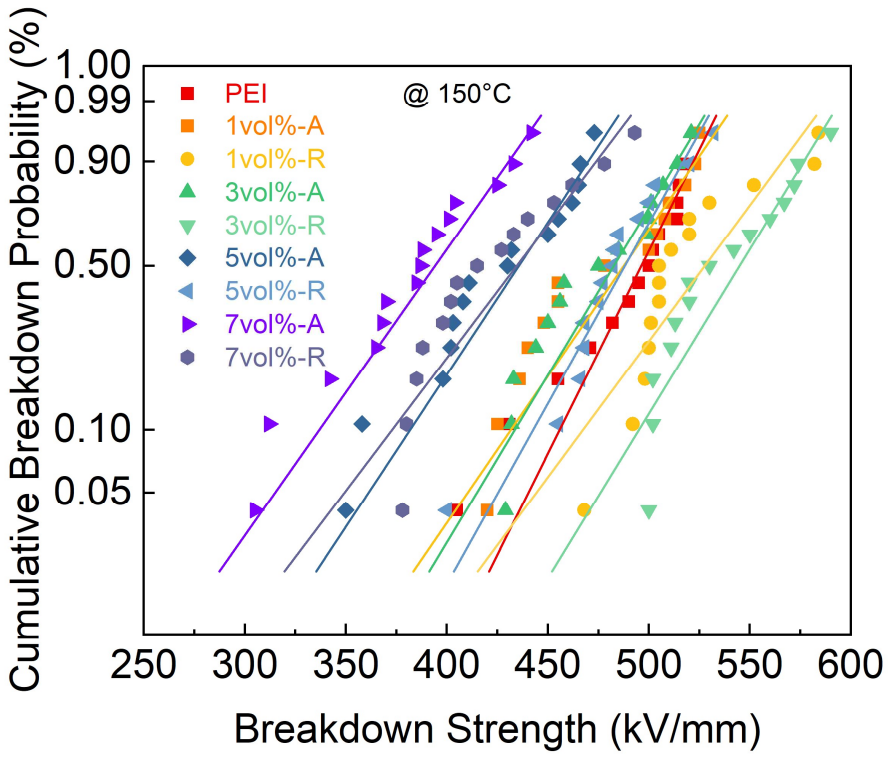

Fig. S10 The two-parameter Weibull statistic of PEI/FTO composite films.

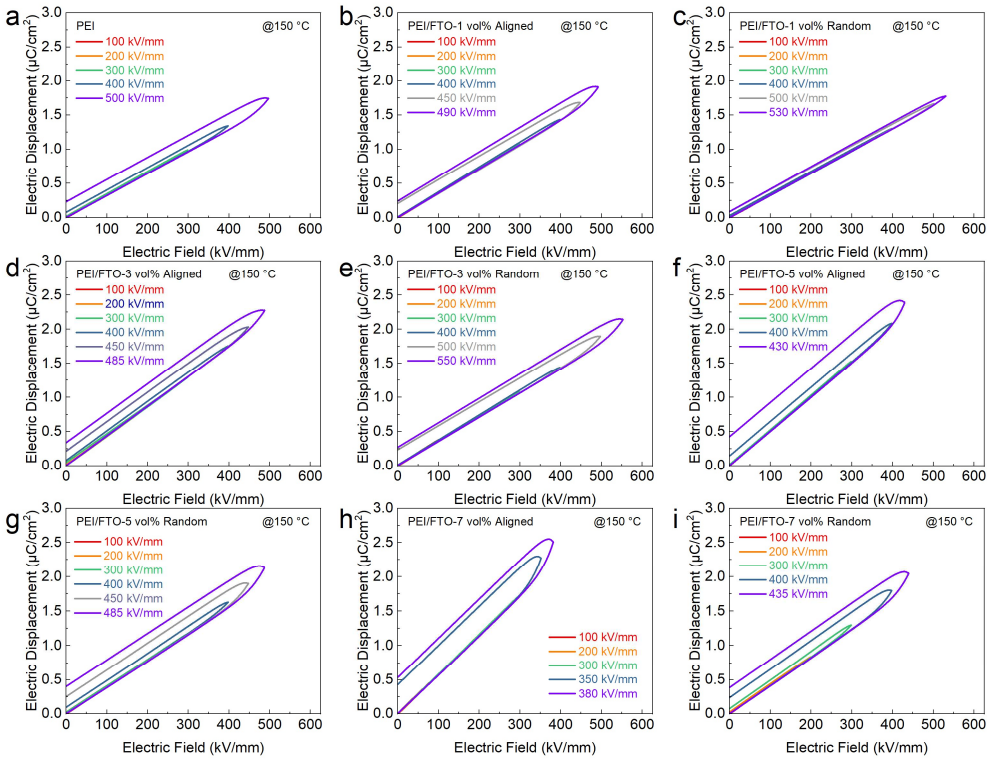

Fig. S11 The electric displacement-electric field loops of PEI/FTO composite films with different nanofibers status at 150 °C.

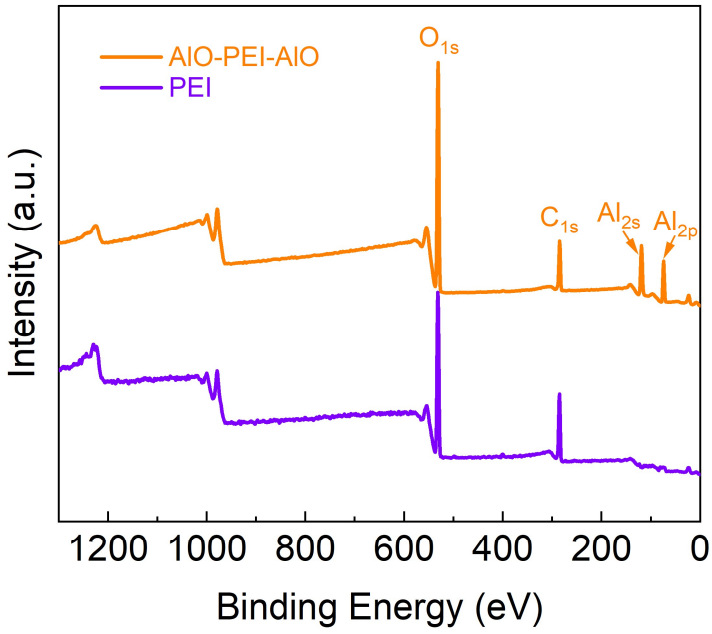

Fig. S12 XPS spectrum of PEI film and AlO-PEI-AlO films.

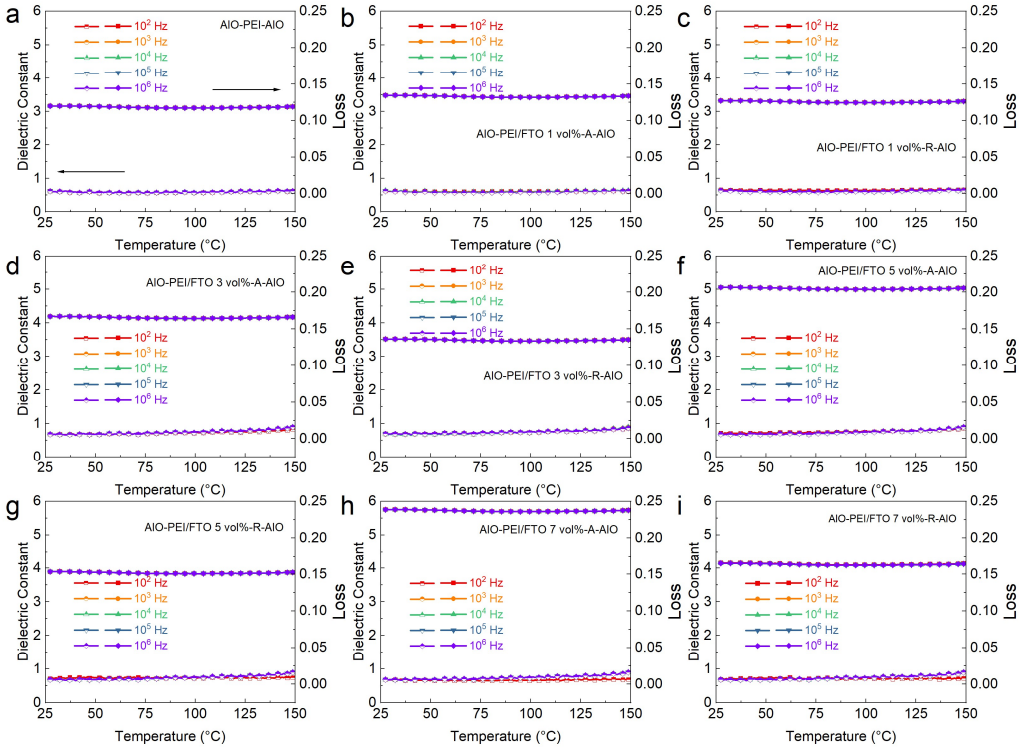

Fig. S13 Dielectric properties as a function of temperature and frequence spectrum of AlO-PEI/FTO-AlO composite films, temperature ranges from 25-150 °C, frequence were set at 10^2, 10^3, 10^4, 10^5 and 10^6 Hz.

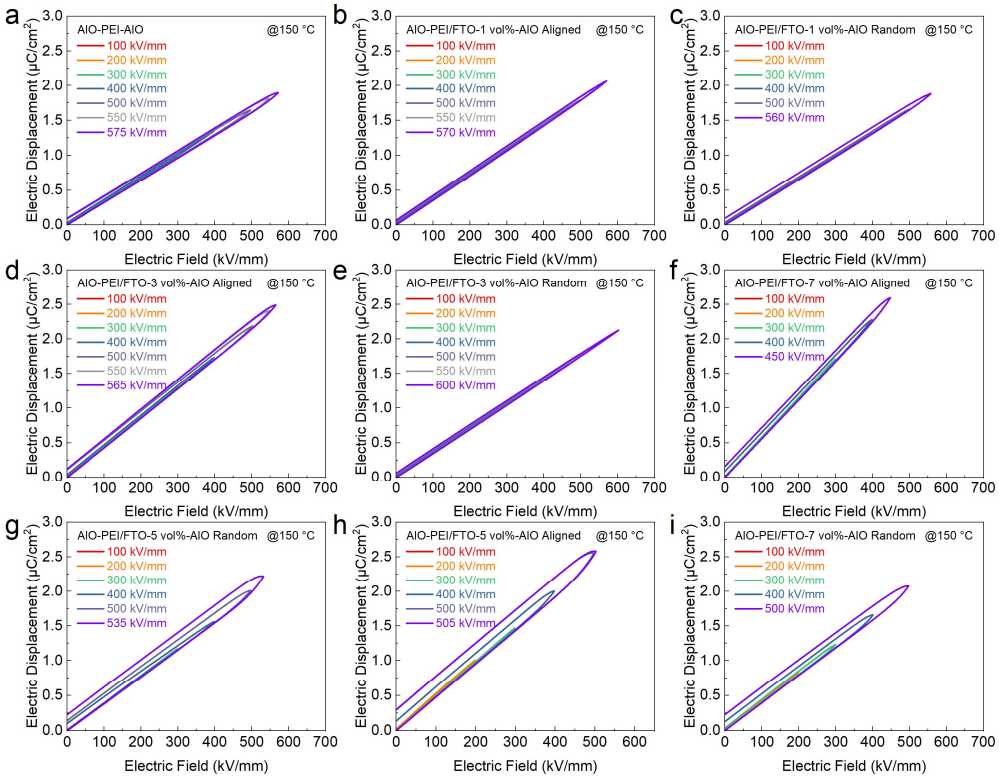

Fig. S14 Electric displacement-electric field (D-E) loops of AlO-PEI/FTO-AlO composite films with different nanofibers contents and status.

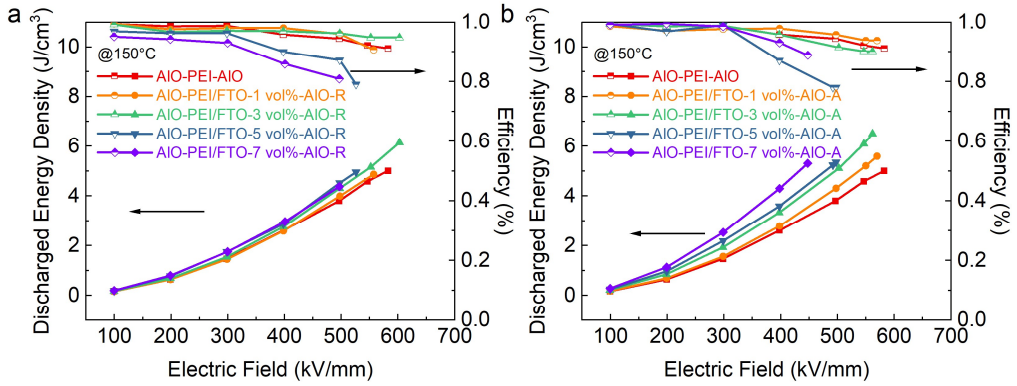

Fig. S15 Discharged energy density of AlO-PEI/FTO-AlO composite films with different nanofibers contents, a) Random films; b) Aligned films.

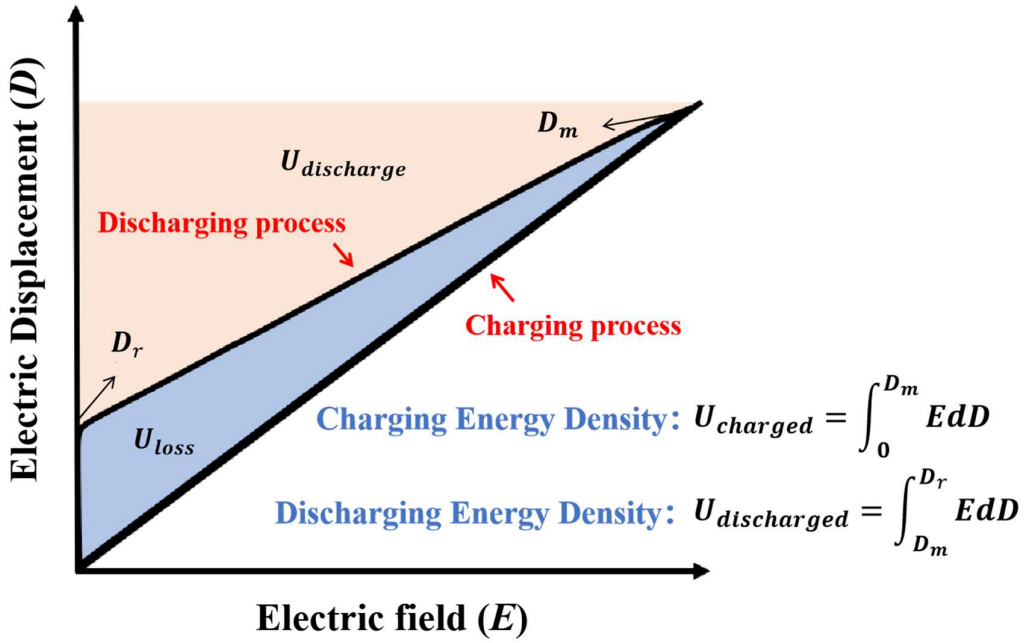

Fig. S16 Schematic diagram of charging and discharging processes of dielectric materials.

Energy Efficiency Calculation

The energy storage performances including charged energy density ($U_{charged}$), discharged energy density ($U_{discharged}$) and energy efficiency (η) are calculated based on the electrical displacement – electric field loops. As shown in Fig R6 and equation 6. The $U_{charged}$ is calculated as, where D_m is the maximum displacement. The $U_{discharge}$ is calculated as, where D_r is the remnant displacement. The η is the ratio of discharged energy density to charged energy density, which can be calculated by:

$$\eta = \frac{U_{discharge}}{U_{charged}} \times 100\% = \frac{\int_{D_m}^{D_r} EdD}{\int_0^{D_m} EdD} \times 100\% \quad (12)$$

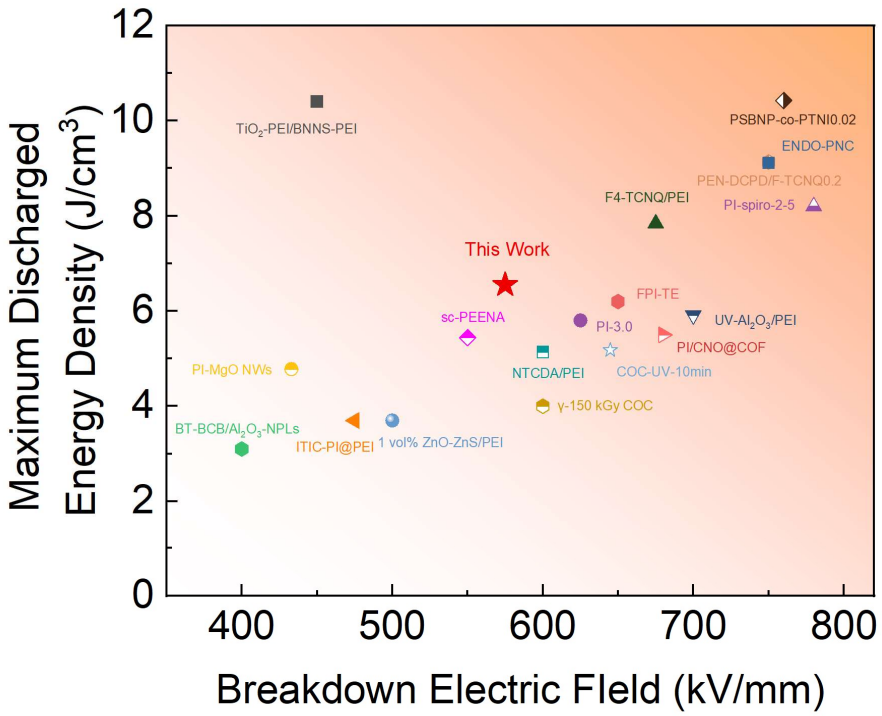

Fig. S17. The maximum discharged energy density *vs.* breakdown electric field of our work compared with previous research.

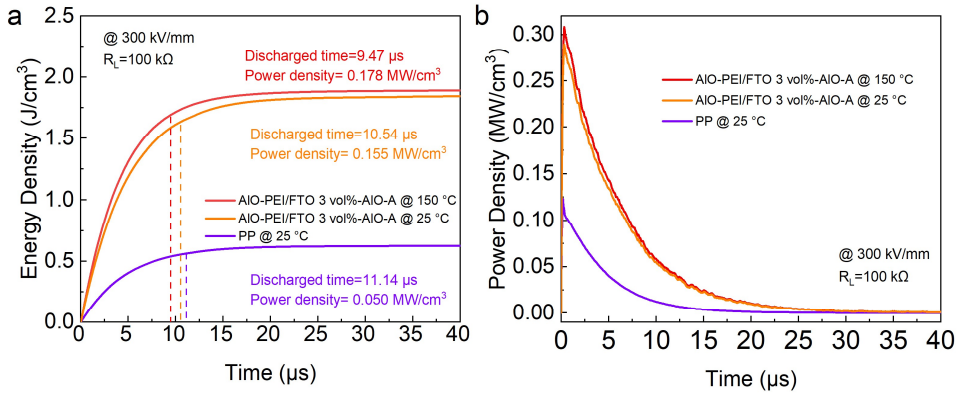

Figure S18. Fast charge and discharge test of AlO-PEI/FTO 3 vol%-AlO-A composite films and BOPP films, a) Energy density; b) Power density.

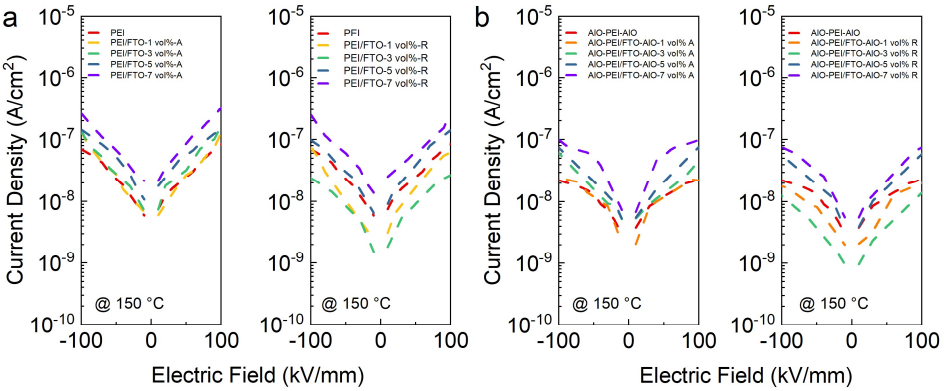

Fig. S19. Leakage current densities of a) PEI/FTO composite films, aligned films (left) and random films (right); b) AlO-PEI/FTO-AlO composite films, aligned films (left) and random films (right).

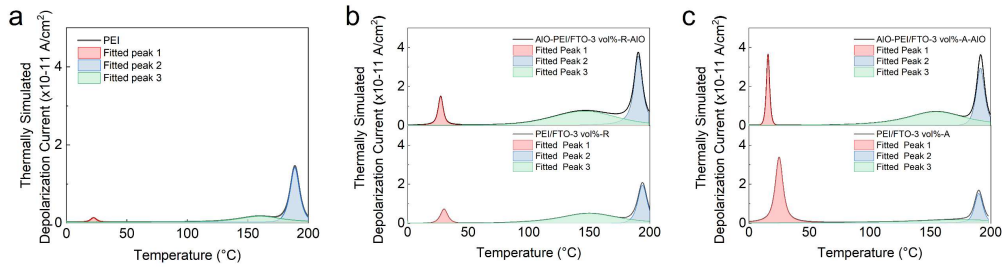

Fig. S20. Thermally stimulated depolarization current (TSDC) measurement of a) PEI films, PEI/FTO 3vol% composite films and AlO-PEI/FTO 3vol%-PEI composite films with different fibers states, b) Random composite films; c) Aligned composite films.

Thermally stimulated depolarization current (TSDC) measurement

The TSDC measurement was carried out by HCTSDC-2000 thermally stimulated depolarization current test system (Beijing Hua Ce Testing Instrument Co., Ltd.). The samples were polarized under an electric field of 20 kV/mm at 180 °C for 10 min, then rapidly cooled down to −100 °C and maintained at this temperature for 10 min. then the films were heated to 200 °C at a rate of 3 °C/min with the depolarization current being recorded.

The charge carrier trapping characteristics of composite films are analyzed, the theoretical process can be expressed as the following equation:

$$ln[I(t)] = a_0\, ln\left(\frac{n}{n_i}\right) + ln(sn_i) - w_0/k_BT \tag{13}$$

where $I(t)$ is the depolarization current curve, a_0 is kinetic order, n is the charge carrier concentration and n_i is the initial concentration of charge carriers in the trap, s is frequency factor, w_0 is the activation energy level of traps, T is the absolute temperature, k_B is the Boltzmann constant.

Extracting three points (T_1, I_1), (T_2, I_2) and (T_3, I_3) from the curve and putting them into the equation:

$$w_0 = \frac{k_B\left[ln\left(\frac{I_3}{I_1}\right) - \frac{ln\left(\frac{n_3}{n_1}\right)}{ln\left(\frac{n_2}{I_1}\right)} l\, n\left(\frac{I_2}{I_1}\right)\right)}{\frac{ln\left(\frac{n_3}{n_1}\right)}{ln\left(\frac{n_2}{n_1}\right)}\left(\frac{1}{T_2} - \frac{1}{T_1}\right) - \left(\frac{1}{T_3} - \frac{1}{T_2}\right)} \tag{14}$$

$$n = \int_T^{T_0} I dT \tag{15}$$

where T_0 is the corresponding temperature while current decays to 0.

The evaluated trap energy level (A_{tsdc}) and trap site density (Q_{tsdc}) can be further calculated as given equation:

$$A_{tsdc} = \frac{2.47 k_B T_p^2}{\Delta T} \tag{16}$$

where T_p is the temperature of the current peaks, and ΔT is the full width at half of the peak.

$$Q_{tsdc} = \frac{60}{v}\int_{T_1}^{T_2} I(T)dT \quad (17)$$

where T_1 is the initial temperature, T_2 is the final temperature, $I(T)$ is the cure of depolarization current and v is the rate of heating.

Table S1. Different peaks, trap energy level, trap site density and activation energy level of traps calculated from TSDC curves for neat PEI, PEI/FTO and AlO-PEI/FTO-AlO with 3 vol% nanofibers in different states.

	Peak 1 (°C)	Peak 2 (°C)	Peak 3 (°C)	A_{tsdc} (eV)	Q_{tsdc} (nC)	W_0 (eV)
PEI	22	156	189	1.55	8.36	0.49
PEI/FTO-R	30	149	194	1.82	19.33	0.53
PEI/FTO-A	25	156	190	1.67	10.28	0.50
AlO-PEI/FTO-AlO-R	27.3	147	191	2.32	24.53	0.58
AlO-PEI/FTO-AlO-A	15.9	157	193	2.18	20.16	0.55

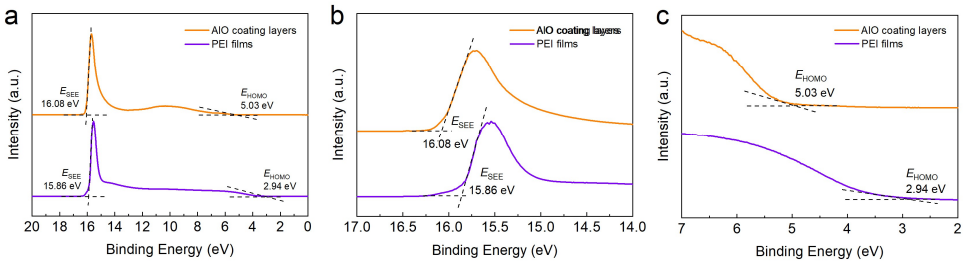

Fig. S21. Ultraviolet photoelectron spectroscopy (UPS) measurement of AlO coating layers and PEI films. The electrons in the occupied energy state are excited by the incident photon energy ($h\nu$=21.22 eV). We can obtain the work function ϕ by calculating the difference between the secondary electron edge (E_{SEE}) and the photon energy. The position of E_{SEE} can be obtained from b). The baseline and the tangents of the curve in the secondary electron edge region. The highest occupied molecular orbital (HOMO) of the dielectrics E_{HOMO} is the minimum binding energy of the photoelectron from the dielectrics. The position of E_{HOMO} can be extracted from c). The baseline and tangents of the curve of the curve in HOMO region.

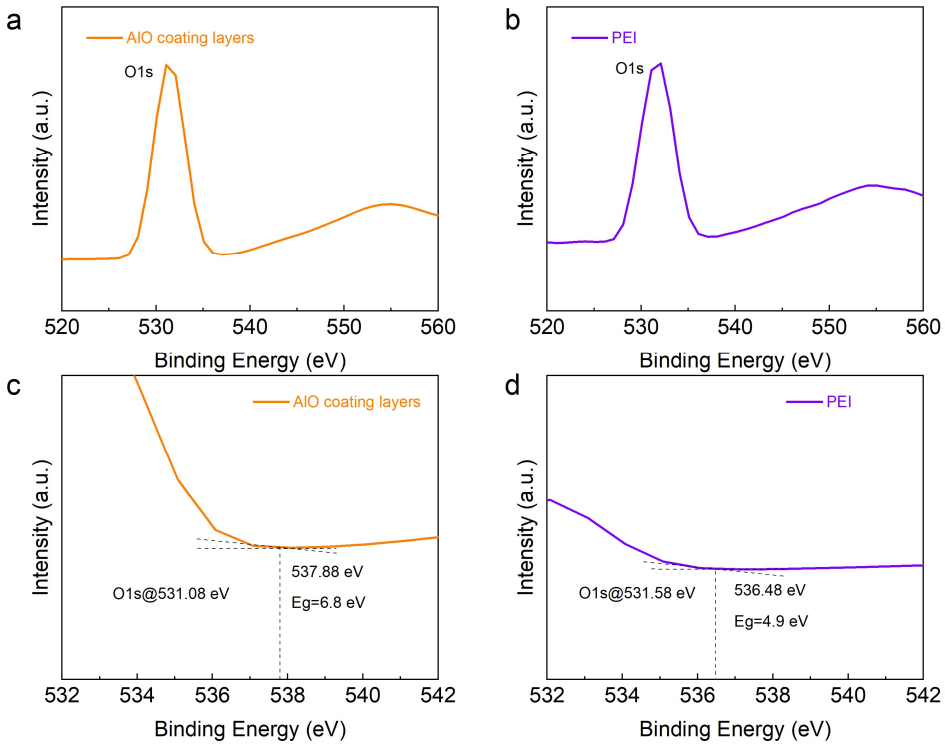

Figure S22. The X-ray photoelectron spectroscopy (XPS) measurement of a) AlO coating layers and b) PEI films, the partial enlarged images are the intensity with the binding energy range from 532-542 eV.

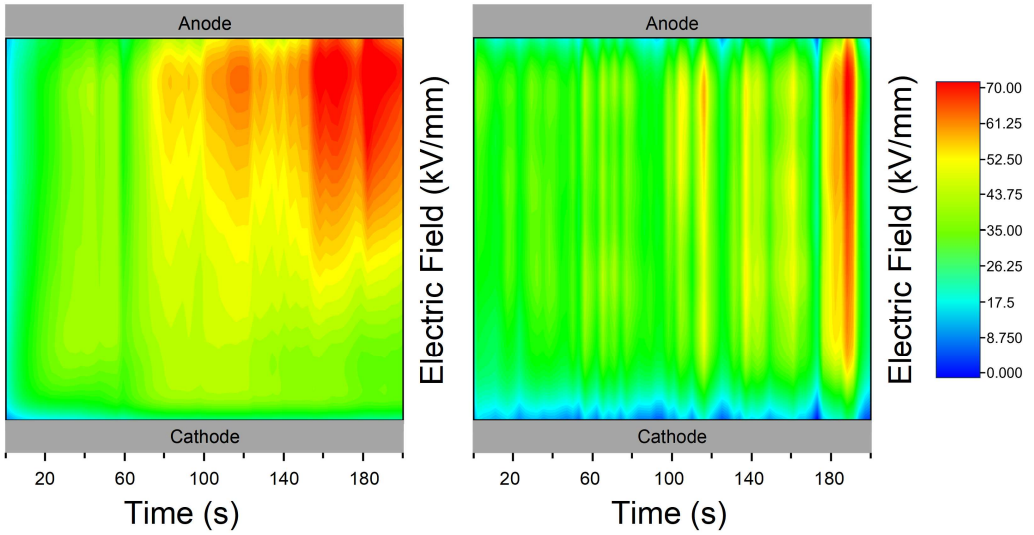

Fig. S23. The electric field distribution of PEA tests on PEI/FTO 3 vol%-A films (left) and AlO-PEI/FTO 3 vol%-A-AlO (right).

References:

1 K. C. Kao, *Br. J. Appl. Phys.*, 1961, **12**, 629.

2 Z. Li, J. Zou, J. Wang, Z. Shen, B. Li, X. Zhang and C.-W. Nan, *Compos. Sci. Technol.*, 2023, **242**, 110209.

3 R. M. Erb, R. Libanori, N. Rothfuchs and A. R. Studart, *Science*, 2012, **335**, 199–204.